Available online at www.sciencedirect.com
ScienceDirect
Bioelectrochemistry 71 (2007) 149–156
Bioelectrochemistry
www.elsevier.com/locate/bioelechem

Effect of shape on the dielectric properties of biological cell suspensions

A. Di Biasio [a], C. Cametti [b,*]

[a] Dipartimento di Fisica, Universita' di Camerino, Camerino, Italy
[b] Dipartimento di Fisica, Universita' di Roma "La Sapienza" Piazzale A. Moro 5, I-00185 — Roma (Italy) and INFM CRS-SOFT, Unita' di Roma1, Italy

Received 16 December 2006; received in revised form 7 March 2007; accepted 7 March 2007
Available online 14 March 2007

Abstract

In this note, we analyze the effect of cell shape on the dielectric and conductometric behavior of biological cell suspension, in a frequency range where the interfacial polarization characteristic of highly heterogeneous systems occurs. We consider two different families of curves, both of them capable of generating a variety of symmetric or asymmetric shapes, ranging from oval, to dog-bone like, to lemniscate curves. These curves, which differ from those generally employed in dielectric models of biological cell suspensions, describe in principle different cells including discocytes, cup-shaped cells, pear-shaped cells, dumbbells and cells with spherical protrusions or invaginations. Our analysis, based on a numerical solution of the Laplace equation by means of boundary element methods, is carried out in the attempt of separating the contributions associated with the different electrical properties of the dielectric media involved from the ones mainly associated with the shape of the cell. We determine the dielectric strength of the dielectric dispersion for a variety of cell shapes and the phenomenological correlation between this parameter of the relaxation and the cell geometry is briefly discussed and commented.

Keywords: Biological membranes; Shape effect; Maxwell–Wagner polarization

1. Introduction

Dielectric relaxation measurements of biological cell suspensions provide a non-invasive method to characterize the average electrical parameters of both the cell membrane and the intracellular and extracellular medium, by means of the evaluation of electrical parameters, such as the permittivity ϵ and the electrical conductivity σ.

The method takes advantage of the fact that, under the influence of an external electric field, the dispersed particles (cells) exhibit a rich fluid-dynamic behavior that can be accounted for by dielectric spectroscopy [1,2], by dielectrophoresis [3,4] or by electrorotation [5] methods. As far as the dielectric spectroscopy methods are concerned, in response to a frequency-dependent electric field, an asymmetric charge distribution at the cell surface is produced, imparting to the cell itself an induced dipole moment whose frequency-dependent relaxation can be easily monitored by means of electrical impedance spectroscopy technique [2,6]. The resulting dielectric response, which yields valuable information on the structural and functional properties of the system, is influenced by many factors, some of them associated with the bulk electrical properties of the different media, some with the surface properties (intrinsic or structural surface charge density) and some others with the geometry of the dispersed objects.

In the framework of the mean-field approximation of heterogeneous systems [7], the primary problem is to arrange an appropriate dielectric model, able to describe the main properties of the system, without introducing a high degree of complexity.

According to the widely accepted dielectric models for biological cell suspension [8–10], each particle (cell) is modeled by a spherical or ellipsoidal core of complex dielectric constant

$$\epsilon_p^*(\omega) = \epsilon_p + \sigma_p/(i\omega\epsilon_0) \quad (1)$$

covered by one or more concentric shells of thickness δ_j and complex dielectric constant

$$\epsilon_{sj}^*(\omega) = \epsilon_{sj} + \sigma_{sj}/(i\omega\epsilon_0)(j = 1,2,..) \quad (2)$$

* Corresponding author. Tel.: +39 06 49913476; fax: +39 06 4463158.
E-mail address: cesare.cametti@roma1.infn.it (C. Cametti).

1567-5394/$ - see front matter © 2007 Elsevier B.V. All rights reserved.
doi:10.1016/j.bioelechem.2007.03.002

The shelled particles are uniformly distributed in a continuous aqueous medium with complex dielectric constant

$$\epsilon^*_{\mathrm{m}}(\omega) = \epsilon_{\mathrm{m}} + \sigma_{\mathrm{m}}/(i\omega\epsilon_0). \quad (3)$$

The fractional volume of the particles is Φ. Here, ϵ_k and σ_k (k=p, s, m) are the permittivity and the electrical conductivity of each medium involved (p, the particle core, s the shell and m the external medium), ω is the angular frequency of the applied electric field and ϵ_0 the dielectric constant of free space. The electrical properties of each medium are characterized by two electrical parameters, ϵ_k and σ_k, both of them considered independent of frequency or, in other words, the frequency of the applied field is well below any eventually occurring characteristic relaxation frequency of each medium.

These dielectric models can be easily extended to more composite systems representing the structure of the cell by assuming spherical or ellipsoidal geometries in which a number of different media (the cytosol, the cell plasmatic and nuclear membranes and the different intracellular media) are arranged as core and shells.

According to this class of models, the expressions for the complex dielectric constant $\epsilon^*(\omega)$ or, equivalently, the complex electrical conductivity $\sigma^*(\omega)$ of the whole suspension can be derived from the knowledge of the electrostatic potential $\Psi(\vec{r})$ which obeys the Laplace equation $\nabla^2\Psi(\vec{r}) = 0$ in each medium. This approach is based on the assumption that the shell membrane behaves as an isotropic dielectric material whose permittivity ϵ_{s} and conductivity σ_{s} are independent of frequency and, moreover, that the charge distributions near each interface have a null thickness (absence of a bulk ionic polarization).

Although this approach is well justified in a variety of biological cell membranes [11–14], when the electrical properties of the interfaces induce different polarization mechanisms which cause additional dielectric dispersions, the above assumptions are no longer valid and the contribution of the bulk ion diffusion in the inner and outer medium must be appropriately taken into account [15,16]. Owing to the diffusion of ions, a finite thickness charge distribution on both sides of each shell arises, influencing the overall interfacial polarization.

In the presence of free charges, the solution of the above stated dielectric model, within the mean-field approximation, requires the knowledge, at every point $\vec{r}$ of the system, of the electrical potential $\Psi(\vec{r})$ or, more correctly, of the mean potential of the mean force fields exerted by all the fixed and mobile charge distributions in the system. This potential obeys the Poisson equation $\nabla^2\Psi(\vec{r}) = -\rho(\vec{r})/\epsilon_0\epsilon_{\mathrm{m}}$ with the appropriate boundary conditions (the continuity of the potential and the normal component of the displacement at the different interfaces), where the electrical charge density $\rho(\vec{r})$ is given by the Boltzmann equation

$$\rho(\vec{r}) \equiv \rho_{\mathrm{f}}(\vec{r}) + \sum_i z_i e n_i(\vec{r}) = \rho_{\mathrm{f}}(\vec{r}) + \sum_i z_i e n_{0i} \exp\left(-\left(z_i e \Psi(\vec{r})\right)/(K_{\mathrm{B}}T)\right) \quad (4)$$

with e as the elementary charge, z_i and $n_i(\vec{r})$ the valence and the concentration of the ith ionic species, $K_{\mathrm{B}}T$ the thermal energy, n_{0i} the concentration of the ionic species in the bulk solution, where the electrical neutrality prevails and $\rho_f(\vec{r})$ the density of the fixed source charges.

The single (or multiple) shell model is based on the assumption that each shell is an isotropic dielectric, non-dispersive, material, i.e., the membrane permittivity ϵ_{s} and the membrane conductivity σ_{s} are independent of the frequency of the applied electric field. The cell membrane of most mammalian cells satisfies there requirements [17,18]. This model has been used to characterize the dielectric properties of a variety of cells and biological object suspensions [19].

However, biological cell shape may differ from a single or multiple shell spherical and/or ellipsoidal geometry and, for these systems, an explicit solution of the Laplace (or Poisson) equation cannot be obtained. Actually, even for shelled ellipsoids, the analytical solution of the Laplace equation would require a shell of non-uniform thickness, since the surface of the shell must be confocal with the surface of the particle core [20]. This circumstance is generally undervalued even if, in some cases, it can markedly influence the overall dielectric behavior.

When the cell shape deviates from a simple geometry, i.e., when the interfaces separating the different media do not coincide with a surface of constant coordinates, within a certain set of coordinate types, we must direct ourselves towards a numerical solution of the electrostatic problem. In these cases, the dielectric response of a cell suspension will contain contribution both from the electrical properties of its constituents and from the cell geometry and it may be not easy to separate each other.

The relative influence of the electrical and geometrical parameters has not been investigated systematically so far and, moreover, the possibility of monitoring alterations of the cell shape from the measurements of the dielectric spectra has not been fully evaluated. On the contrary, in many biotechnological processes [21,22], the possibility of controlling, in a non-invasive manner, biological function by means of electrical methods may be of relevant importance [23–25].

In this note, we focus on the influence of the cell geometry, when it deviates from the simple spherical or ellipsoidal form, on the dielectric response of a biological cell suspension. We will consider two families of curves able to generate axis-symmetric objects that can simulate a variety of biological cells or, in different conditions, cells during the different stage of growth. By means of numerical solution of the Laplace equation, using the boundary element method, we have simulated the dielectric relaxation due to the interfacial polarization in cases characterized by cells of different shapes, well different from a spherical or ellipsoidal shape. A phenomenological correlation between the dielectric strength of the relaxation and the cell shape is briefly discussed and commented.

2. The boundary element method

The Laplace equation $\nabla^2\Psi(\vec{r}) = 0$ furnishes relatively simple analytical solutions only in the case of spherical or ellipsoidal geometry, in the limit of small cell concentration. An alternative approach has been proposed by Lei et al. [26] by using a spectral representation which offers the advantage of separating electrical parameters from structural and geometrical parameters.

For more realistic cell shapes, in both cases, the electrostatic problem is more complex and must be solved numerically [27–31].

Recently, Sekine [32] has taken into account the real shape of a biological cell by applying the boundary element method [BEM] to the calculation of the electrical potential $\Psi(\vec{r})$ outside a particle, under the influence of an uniform external electric field $E_0(\vec{r}) \equiv (E_{0x}, E_{0y}, E_{0z})$.

This method is a numerical technique that, due to its flexibility and to the efficient solutions obtained over other different techniques, such as the standard finite difference method [FDM] or finite element method [FEM], can be applicable to a wide range of physical and engineering problems. Its main advantage resides in the fact that only the boundary of the domain of the partial differential equation governing the problem to be solved requires the discretisation of the domain into subregions, thus reducing the effective dimension of the problem by one. In particular, when the domain is exterior to the boundary as in the case of the Laplace equation for the cell geometry considered here, this advantage is even more evident since the equation governing the infinite domain is reduced to an equation over the boundary.

In this context, the effective medium theory approximation [7] furnishes the final expression for the complex dielectric constant of the suspension. In particular, assuming a shell with a thickness d is negligible small compared with the cell size and the electric field inside the membrane thickness to be uniform, Sekine [32] has shown that the electrical potential $\Psi_m(r)$ in the external medium can be written in terms of the particle polarizability $P_{x,y,z}$ according to the relationship

$$\Psi_m(r) = \left(P_x x E_{0x} + P_y y E_{0y} + P_z z E_{0z}\right) \frac{1}{r^3} \tag{5}$$

satisfying the boundary conditions (continuity of the potential and the normal component of the displacement at the inner and outer membrane interfaces). Owing to the assumptions adopted, these conditions read

$$\Psi_s|_\Sigma = \Psi_m|_S + \epsilon_m^*/\epsilon_s^* \, d\partial\Psi_m/\partial r|_S \tag{6}$$

$$\epsilon_p^* \partial\Psi_p/\partial r|_\Sigma + \epsilon_m^* \partial\Psi_m/\partial r|_S = 0 \tag{7}$$

where $\Psi_p(\vec{r})$, $\Psi_s(\vec{r})$ and $\Psi_m(\vec{r})$ are the electrical potentials in the cytoplasm, membrane and extracellular medium, respectively and Σ is the boundary cytoplasm–membrane surface and S the boundary membrane–external medium surface. Since the same functional form of Eq. (5) can be derived analytically from the Laplace equation in the case of ellipsoidal particles [33], equating these two equations results in the usual mixture equation, within the effective medium theory approximation.

The boundary element method is based on the discretisation of an integral equation that is mathematically equivalent to the Laplace equation using Green's theorem and that is defined on the boundary of the domain

$$\Psi(\bar{r}) = \oint \left(G(\bar{r}, \bar{r'}) \frac{\partial\Psi(\bar{r'})}{\partial n} - \frac{\partial G(\bar{r}, \bar{r'})}{\partial n} \Psi(\bar{r'}) \right) dA \tag{8}$$

where the surface integral is over the bounding surface of the cell, $\partial/\partial n$ is the component of the gradient in the direction of the outward-pointing normal to the surface and $G(\bar{r}, \bar{r'}) = 1/(4\pi|\bar{r} - \bar{r'}|)$ is the Green function for the Laplace equation. In the present case, i.e., an object covered by a thin shell, the discretisation of the domain surface applies only to the outer surface of the cell, because of the boundary conditions that the electrical potential and the electrical field must satisfy at the interfaces between the internal medium and the membrane and between the membrane and the external medium.

Following the method developed by Sekine [32], we have considered the different cell shapes, generated by rotating along an appropriate axis two families of equations, a parametric equation previously proposed by Gheorghiu [34,35] and the Cassini oval [36,37].

The numerical solution of the Laplace equation is calculated considering the particle surface divided into 8×8 isoparametric elements, resulting in a system of $2n$ complex coefficients linear equations, whose solution furnishes the value of the potential and of the electric field at the cell surface, in the center of each element. Once these values are known, the electric potential in the external medium at a distance large enough from the cell surface can be easily evaluated, which gives the final mixture equation for the heterogeneous system.

In the following, we report the main characteristics of the dielectric dispersions in the different cases investigated.

3. Shape with an axial symmetry

A large class of shape of biological objects with an axial symmetry [34,35] can be described in a parametric form by the equation

$$\rho(\vartheta) = A + B\cos\vartheta + C\cos^2\vartheta \tag{9}$$

where A, B and C are parameters which allow various cell shapes, from a sphere to a strangled prolate ellipsoid. The curves can be rotated around their symmetric axis, giving axisymmetric surfaces, which determine the shape of the cell. Eq. (9) (with $A = 1$) has been previously employed by Vrinceann and Gheorghiu [35] in their attempt of studying the shape effect on the dielectric behavior of arbitrarily shaped particle suspensions. This equation is able to furnish both symmetric and asymmetric shaped particles and we will consider separately the symmetric ($B = 0$) and asymmetric ($B \neq 0$) case.

3.1. Symmetric case, $B = 0$

Typical cell shapes, calculated on the basis of Eq. (9), are shown in Fig. 1, for different values of the parameters A and C. The shape varies from a single sphere (upper panel), to an oval, up to a lemniscate (medium panel) and finally to two separate spheres (bottom panel) with the increase of the value of the parameter C from $C = 0$ to about $C = 2$. The value of the other parameter A has been chosen in order to have objects obtained by rotating the curve around its symmetric axis of the same volume, so that the fractional volume Φ of the dispersed phase in the cell suspension is maintained constant throughout the different comparisons.

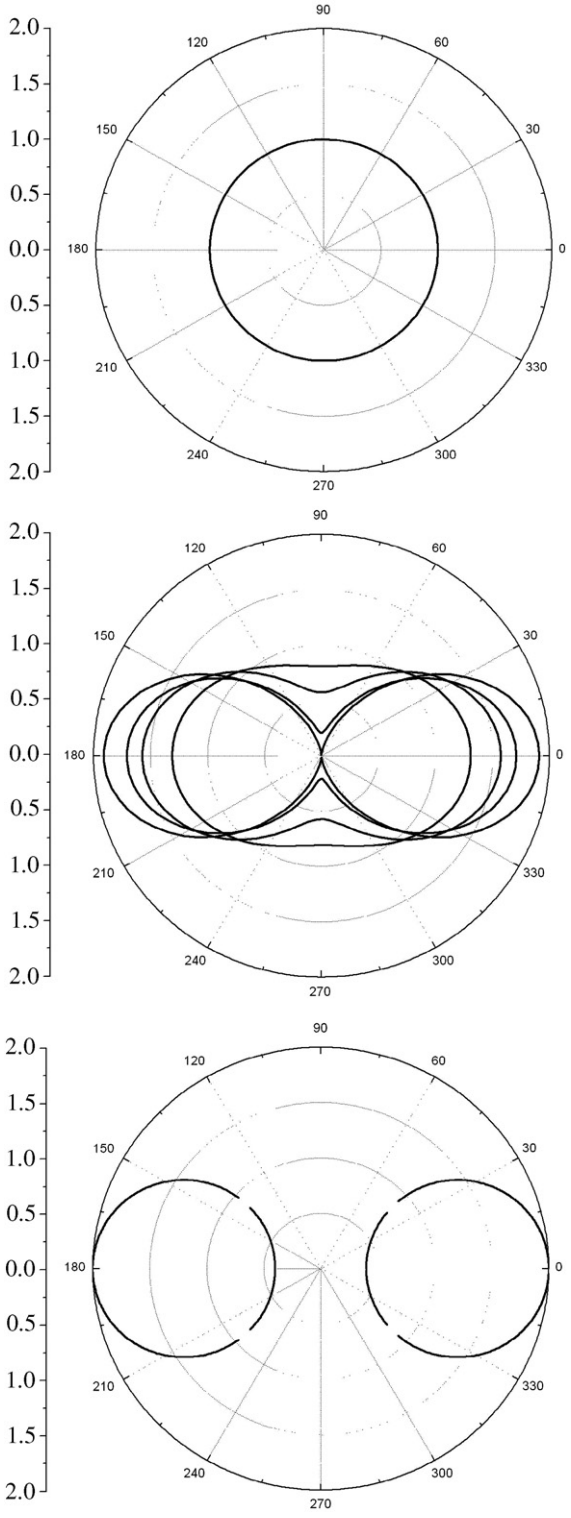

Fig. 1. Cross-section of the cells whose contour is determined by Eq. (9) with $B=0$ and characterized by the following values of the other two parameters: Upper panel: $A=1$, $C=0$. Middle panel: $A=0.8104$, $C=0.50$; $A=0.5719$, $C=1.0$; $A=0.2801$, $C=1.5$; $A=0.0092$, $C=1.9$ from oval to lemniscate figure, respectively. Bottom panel: $A=0.80$, $C=0$. The center of the two spheres are shifted to the abscissas $(-1.2,0)$ and $(1.2,0)$, respectively, for clarity of presentation. The curves can be rotated around their symmetric x axis, giving axisymmetric surfaces which determine the shape of the cell. The parameters have been chosen in order to obtain particles of the same volume. The labels refer to the polar coordinates ρ and ϑ. The radial coordinate ρ is in arbitrary units.

The numerical simulation of the dielectric behavior of a cell suspension has been carried out with the following values of the dielectric parameters of the cell core, of the cell membrane and of the extracellular medium: $\epsilon_p=80$, $\sigma_p=10^{-2}$ mho/m; $\epsilon_s=5$, $\sigma_s=10^{-6}$ mho/m; $\epsilon_m=80$, $\sigma_m=10^{-2}$ mho/m, respectively. The fractional volume of the dispersed phase is fixed to the value $\Phi=0.1$ and the ratio δ/R between the membrane thickness and the average size of the cell is assumed $\delta/R=0.005$. The choice of these values is justified by the aim to magnify the influence of the shape on the overall dielectric response. To this end, we have assigned the same values, both the permittivity and the electrical conductivity, to the intracellular medium (cytosol) and to the extracellular medium.

Typical dielectric and conductometric spectra are shown in Fig. 2, where each curve, corresponding to a single cell shape, evidences how the dielectric dispersion depends on the geometry of the dispersed object. The spectra show a rather complex structure, with the progressive appearance of further relaxation processes located in the low-frequency interval, as the cell geometry deviates from the one of a simple sphere to the ones of a pear or of a dumbbell. Overlooking these aspects, which are anyway relevant, we here will focus on the total dielectric strength $\Delta\epsilon$ of the dielectric spectra, considered as the parameter which is mostly influenced by the cell shape.

Fig. 3 shows the low-frequency limit of the permittivity $\epsilon(\omega)$, and hence the dielectric increment $\Delta\epsilon$, as a function of the parameter C. Close to each value, we show a sketch of the cell shape. As can be seen, we observe a marked increase of the dielectric strength of the dispersion, particularly relevant if we consider how much the shell shape is distorted towards a more or less lemniscate or pear forms. This is probably due to the fact that interface polarization experiences the effects of a local curvature which progressively increases for nonspherical shapes. When the cell splits into two separate spheres, maintaining constant the fractional volume Φ, the dielectric strength reduces again. It must be noted that, despite the fact that the fractional volume Φ does not change, in this case the dielectric strength is smaller than the one corresponding to a single sphere. This can be due to

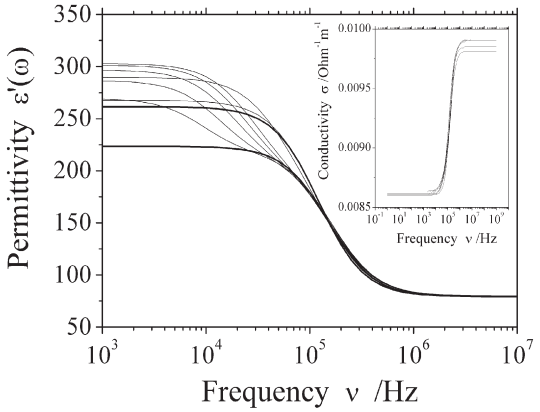

Fig. 2. The permittivity $\epsilon'(\omega)$ as a function of frequency for cells whose shape is sketched in Fig. 1. The higher thicker line corresponds to a single spherical cell (Fig. 1, upper panel) and the lowest thicker line (Fig. 1, bottom panel) to two separate spherical cells of the same overall volume.

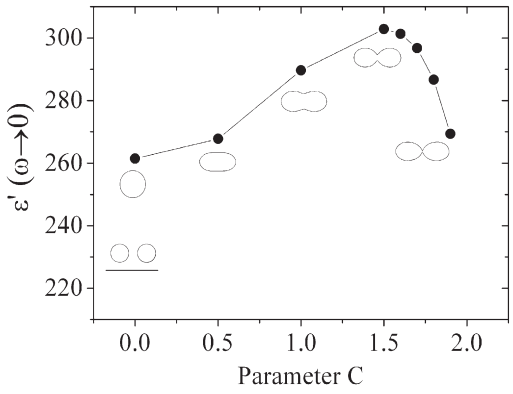

Fig. 3. The low-frequency limit of the permittivity $\epsilon'(\omega)$ for different values of the parameter C. Close to each value, the corresponding cell shape is shown, according to Eq. (9). The values of the parameters are reported in the legend of Fig. 1. The full line represents the value reached by the permittivity when a single sphere is split into two separate spheres of the same overall volume.

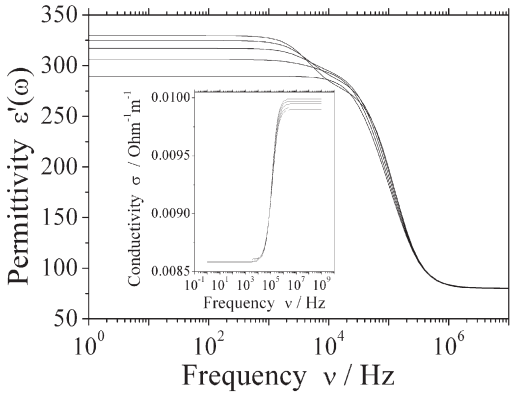

Fig. 5. The permittivity $\epsilon'(\omega)$ as a function of frequency for each of the shell shape shown in Fig. 4. The curves are simulated with the same values of the dielectric parameters as those employed in the symmetric case and the fractional volume of the dispersed phase is $\Phi=0.1$. The values of the shape parameters are the same as those reported in Fig. 4. The inset show the corresponding values of the electrical conductivity $\sigma(\omega)$.

the fact that, as pointed out by Sebastian et al. [38], the presence of a low conductivity membrane (with a conductivity several orders of magnitude lower than those of the cytoplasm and of the physiological extracellular solution) implies that most of the electric field and energy within the cell are concentrated in the membrane.

3.2. Asymmetric case, $B \neq 0$

Eq. (9) furnishes, as well, a family of asymmetric curves. A typical example is shown in Fig. 4, where the parameters A and B have been appropriately varied in order to maintain fixed, also in this case, the volume of the corresponding solids obtained by rotating the curve around the x axis. For simplicity, the value of the third parameter C is maintained constant to the value $C=1$.

In this case, the spectra result, to a first approximation, from a single relaxation process, the presence of a further relaxation falling very close to the main relaxation process (Fig. 5). The overall dielectric dispersion is characterized by a dielectric increment $\Delta\epsilon$ that progressively increases going on from an oval to an approximately spherical shape with an extrusion. This behavior is clearly evidenced in Fig. 6, where close to the single value of $\Delta\epsilon$, the corresponding cell shape is sketched.

Under the same conditions ($B \neq 0$), we analyzed the dielectric behavior of the cell suspension by redoubling the volume of the single dispersed object, maintaining constant the value of the fractional volume. In this way, it is possible to extend the range of the values of the parameters A and B (maintaining the parameter C to the value $C=1$) in order to evidence a larger variety of shapes. The results are summarized in Fig. 7, where we report the dielectric spectra, and in Fig. 8, where the dielectric strength is shown for the different shapes investigated.

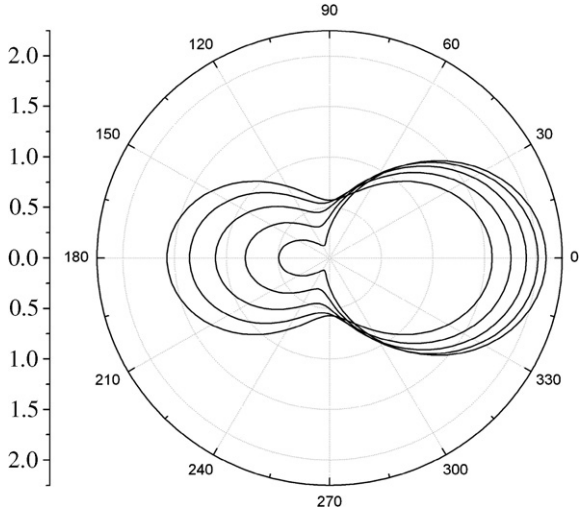

Fig. 4. Cross-section of the cells whose contour is determined by the function Eq. (9) with $B \neq 0$ and characterized by the following values of the other two parameters: $A=0.5719$, $B=0$, $C=1.00$; $A=0.5545$, $B=0.20$, $C=1.00$; $A=0.5024$, $B=0.40$, $C=1.00$; $A=0.4146$, $B=0.60$, $C=1.00$; $A=0.2924$, $B=0.80$, $C=1.00$, from the outer to the inner curve, respectively. The curves can be rotated around their symmetric x axis, giving axisymmetric surfaces which determine the shape of the cell. The labels refer to the polar coordinates ρ and ϑ. The radial coordinate ρ is in arbitrary units.

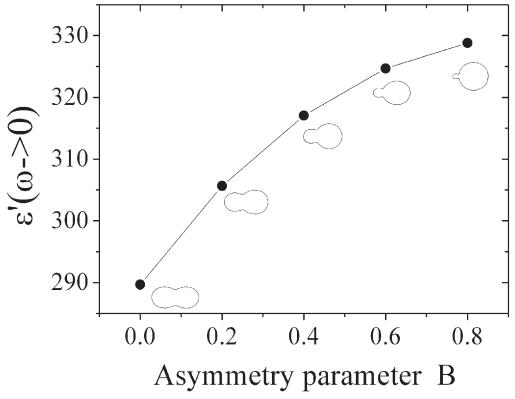

Fig. 6. The low-frequency limit of the permittivity $\epsilon'(\omega)$ for different values of the parameter B. Close to each value, the corresponding cell shape is sketched.

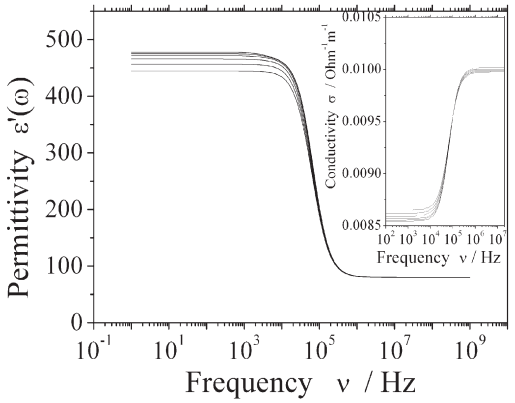

Fig. 7. The permittivity $\epsilon'(\omega)$ as a function of frequency for each of the shell shape shown in Fig. 4. The curves are simulated with the values of the dielectric parameters equal to those employed in the symmetric case and the fractional volume of the dispersed phase is $\Phi=0.1$. The values of the shape parameters are $A=1.621$, $B=0$, $C=1.00$; $A=1.604$, $B=0.30$, $C=1.00$; $A=1.552$, $B=0.60$, $C=1.00$; $A=1.466$, $B=0.90$, $C=1.00$; $A=1.345$, $B=1.20$, $C=1.00$; $A=1.191$, $B=1.50$, $C=1.00$. The corresponding curves run from bottom to top. The inset show the corresponding values of the electrical conductivity $\sigma(\omega)$.

Here, only one dielectric dispersion is evidenced, even if its dielectric increment is significantly larger than the one shown in Fig. 6, for comparable values of the parameter B.

4. Shape governed by a Cassini curve

The Cassini ovals are a family of quartic curves described by a point such that the product of its distances from two fixed points at a distance $2a$ apart is a constant b^2. The shape of the curve varies according to the ratio b/a, generating a single loop (*oval* or *dog bone*) if $a/b<1$, a lemniscate if $a/b=1$ or two separate loops if $a/b>1$. The Cassini ovals have the polar equation

$$r^4 + a^4 - 2a^2r^2\cos(2\vartheta) = b^4. \qquad (10)$$

Some typical curves generated from the Cassini equation are given in Fig. 9, for different values of the parameters a and b (in the case where $a/b<1$). The corresponding dielectric spectra

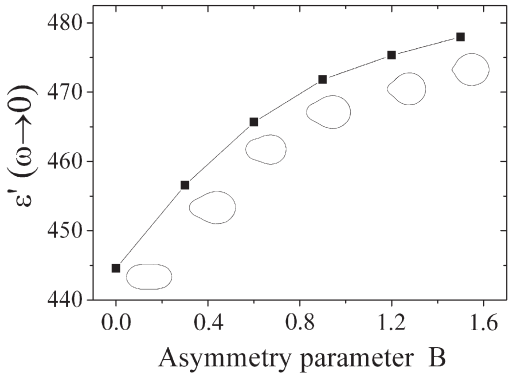

Fig. 8. The low-frequency limit of the permittivity $\epsilon'(\omega)$ for different values of the parameter B. Close to each value, the corresponding cell shape is sketched. The values of the parameters are listed in the caption of Fig. 7.

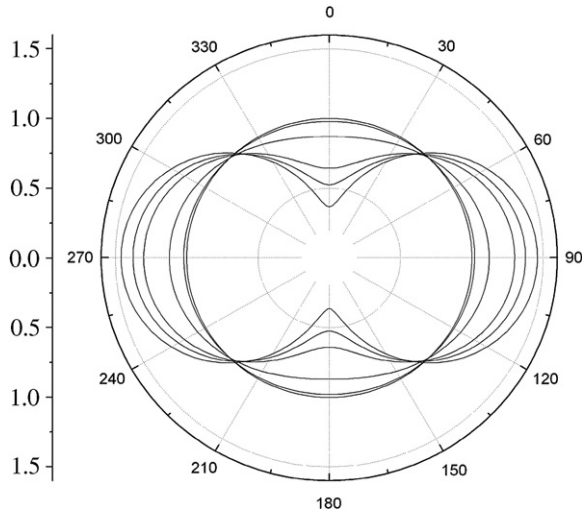

Fig. 9. Cross-section of the cells obeying the Cassini equation (Eq. (10)) for different couples of the parameters a and b: from spherical to dog-bone like shape: ($a=0$, $b=1.000$); ($a=0.20$, $b=1.0001$); ($a=0.5$, $b=1.0035$); ($a=0.8$, $b=1.0251$); ($a=0.9$, $b=1.0412$); ($a=1.0$, $b=1.0642$). The values of the parameters are chosen in order to have the objects of the same volume. The labels refer to the polar coordinates ρ and ϑ. The radial coordinate ρ is in arbitrary units.

are reported in Fig. 10 and the low-frequency limit of the dielectric strength is reported in Fig. 11.

It is worth noting that the shape derived from the Cassini equation, or one of its modified versions, has been employed by different authors [39,40] to describe the erythrocyte shape. More recently, Kralj-Iglič et al. [41] have extensively discussed the equilibrium shape of bilayer vesicles by using a modified Cassini function (with four parameters) and have determined the values of the model parameters from the geometrical constrains for the cell volume and area and by minimizing the membrane bending energy. This general approach yields many different cell shapes, ranging from discocytes, pear-shaped cells, dumbbell cells to cells with spherical protusions and invaginations.

In the present case and in its simplest version, the Cassini equation has the advantage to depend on two parameters only, which provides the freedom needed to vary the cell shape (from

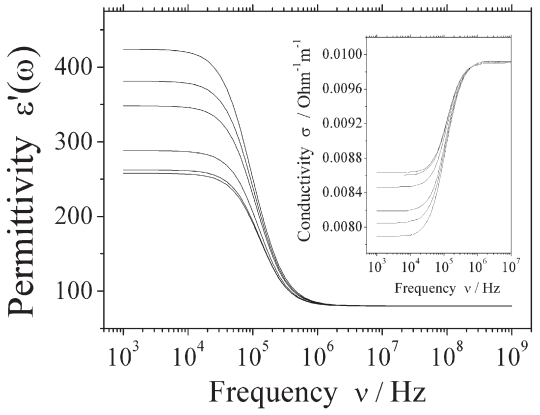

Fig. 10. The permittivity $\epsilon'(\omega)$ as a function of frequency for each of the shell shapes shown in Fig. 9. The values of the parameters are given in Fig. 9. The inset show the corresponding values of the electrical conductivity $\sigma(\omega)$.

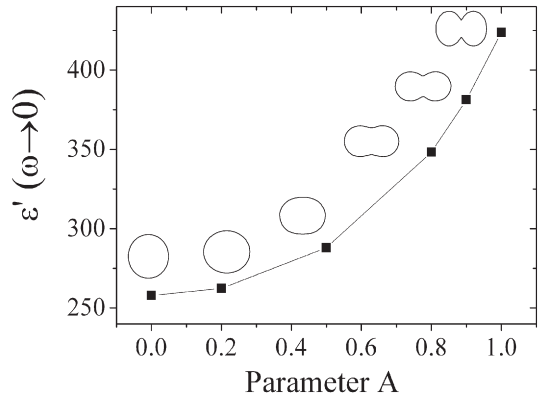

Fig. 11. The low-frequency limit of the permittivity $\epsilon'(\omega)$ for different values of the parameters a and b. Close to each value, the corresponding cell shape is shown.

a biconcave to a spheroidal particle, as requested to describe an erythrocyte cell). In isotonic solutions, measurements of the erythrocyte dimensions carried out by means of optical microscopic determination [39,42] gave the following values: average diameter (7.82±0.42 μm), average minimum thickness (0.81±0.35 μm), average maximum thickness (2.58±0.27 μm), cell volume (94±14 μm^3), and cell surface (135±16 μm^2). This peculiar shape can be described with good accuracy by the oval of Cassini. In particular, these values can be made consistent with the minimum thickness of the cell, given by $u = 2\sqrt{b^2-a^2}$, with the maximum thickness, given by $l = 2\sqrt{a^2-(b^2/2a)^2}$ and with the diameter, given by $v = 2\sqrt{b^2+a^2}$. An analysis of the influence of a cell shape governed by a Cassini equation has been discussed in a recent work [43].

5. Discussion

In the framework of an overall spheroidal geometry, Asami et al. [44] have clearly demonstrated how the dielectric response depends on the shape of the cell. This feature is clearly evidenced, for example, in the case of three different biological structures, such as swollen spherical erythrocytes, lymphoma cells and plant protoplasts, where, beside the basic dispersion of the spherical structure, additional dispersions result from interfacial polarization of nuclear membrane and intracellular organelles, from the presence of vacuoles and from the cytoplasmic layer containing chloroplasts, respectively.

In contrast to spherical geometry, only a few investigations deal with nonspherical cells. We can mention here the studies on the budding yeast cells as doublet structures [45] and a study on rod-shaped *Escherichia coli* cells [46]. More recently, the influence of the cell shape in the evolution of a suspension of initially synchronized budding yeast cells has been studied by Gheorghiu and Asami [47]. Finally, a further example rises from the dielectric behavior of cell suspensions formed by a mutant of fission yeast cells during the division cycle, investigated by Asami [48]. In this case, the dielectric response has been analyzed as due to three consecutive, partially overlapping, dielectric dispersions. The cells are modeled as prolate spheroids which axial ratio varies according to the cultivation phase. This study provides a method to determine the morphological parameters from the dielectric response. At last, the application of the dielectric methods in the monitoring of the rouleaux formation in human blood carried out by Irimajiri et al. [49] deserves to be mentioned.

On the other hand, the Cassini equation, with the two free parameters a and b chosen to model the diameter and the least thickness respectively of red blood cells, has been employed by Gheorghiu [40], in his analysis of the applicability of the ellipsoidal model.

However, the cell morphology may markedly differ from the one of a more or less simple spherical or ellipsoidal geometry, giving rise to changes in the interface polarization effects. The influence of the cell shape on the dielectric response of biological cell suspensions suggests that dielectric spectroscopy methods may represent a promising technique to monitor a variety of functions of biological systems, such as cell cycle progression, where there is a continuous cell shape change.

The effect of geometry of arbitrarily shaped cells on the overall dielectric response can be well evidenced in the case of shelled particles with the inner medium exhibiting the same electrical properties of the extracellular medium. In this way, the effects associated to the geometry can be separated from the ones mainly influenced by the electrical properties of the adjacent media. We have presented a phenomenological correlation between the dielectric increment of the dielectric dispersion and the geometrical parameters that govern the overall shape of the dispersed particles. The dielectric spectra have a rather complex behavior due to the presence of multiple relaxation, partially overlapping, effects, induced by the peculiar shape considered. However, neglecting these effects and focusing on the total dielectric increment, that can be easily measured experimentally, we have simulated its value for a suspension of largely arbitrarily shaped cells. These results show that, for a largely class of shapes, beyond electrical parameters, it is possible to extract from the experimental data, relevant geometric parameters, joined with different biological events in the cellular growth. Taking into account that in various processes cell shape often differs from a spherical or ellipsoidal geometry, the knowledge of its influence on the overall dielectric response of the cell suspension allows to monitor different biological events such as the cell cycle progression or other important aspects of the cell dynamics.

Acknowledgment

We wish to acknowledge the support of INFM-CNR CRS-SOFT.

References

[1] R. Pethig, D.B. Kell, The passive electrical properties of biological systems: their significance in physiology, biophysics and biotechnology, Phys. Med. Biol. 32 (1987) 938–970.
[2] K. Asami, Characterization of heterogeneous systems by dielectric spectroscopy, Prog. Polym. Sci. 27 (2002) 1617–1659.

[3] G. Fuhr, I. Kuzmin, Behavior of cells in rotating electric fields with account to surface charge and cell structures, Biophys. J. 50 (1985) 789–795.
[4] H.A. Pohl, Dielectrophoresis, Cambridge Univ. Press., Cambridge, 1978.
[5] J. Gimsa, P. Marszalek, U. Loewe, T.Y. Tsong, Dielectrophoresis and electrorotation of neurospore sline and murine myeloma cells, Biophys. J. 60 (1991) 749–760.
[6] K.R. Foster, H.P. Schwan, Dielectric properties of tissues in: C. Polk, E. Postow (Eds.), Handbook of Biological Effects of Electromagnetic Fields, CRC Press, Boca Raton, 1996, pp. 25–107.
[7] M. Clausse, Dielectric properties of emulsions and related systems, in: P. Becher (Ed.), Encyclopedia of Emulsion Technology. Basic Theory, Marcel Dekker, New York, 1983, pp. 481–715.
[8] K. Asami, Y. Takahashi, S. Takashima, Dielectric properties of mouse lymphocytes and erythrocytes, Biochim. Biophys. Acta 1010 (1989) 49–55.
[9] K. Asami, T. Yamaguchi, Dielectric spectroscopy of plant protoplasts, Biophys. J. 63 (1992) 1493–1499.
[10] V. Raicu, T. Saibara, A. Irimajiri, Dielectric properties of rat liver in vivo: Analysis of modeling hepatocytes in the tissue architecture, Bioelectrochem. Bioenerg. 47 (1998) 333–347.
[11] R. Licin, B.-Z. Ginzburg, M. Schlesinger, Y. Feldman, Time domain dielectric spectroscopy study of human cells. I — erythrocytes and ghosts, Biochim. Biophys. Acta 1280 (1996) 34–40.
[12] H. Beving, L.E.G. Eriksson, C.L. Davey, D.B. Bell, Dielectric properties of human blood and erythrocytes at radio-frequencies (0.2–10 MHz). Dependence on cell volume fraction and medium composition, Eur. Biophys. J. 23 (1994) 207–215.
[13] C. Ballario, A. Bonincontro, C. Cametti, A. Rosi, L. Sportelli, Conductivity of normal and pathological human erythrocytes (homozygous beta-thalassemia) at radiowave frequencies, Z. Naturforsch. 39C (1984) 160–166.
[14] F. Bordi, C. Cametti, A. Rosi, A. Calcabrini, Frequency domain electrical conductivity measurements of the passive electrical properties of human lymphocytes, Biochim. Biophys. Acta 1153 (1993) 77–88.
[15] V.N. Shilov, A.V. Delgado, F. Gonzales-Caballero, C. Grosse, Thin double layer theory of the wide-frequency range dielectric dispersion of suspensions of non-conducting spherical particles including surface conductivity of the stagnant layer, Colloids Surf., A Physicochem. Eng. Asp. 192 (2001) 253–265.
[16] C. Grosse, Dielectric properties of suspensions of solid particles, in: T.A. Hubbard (Ed.), Encyclopedia of Surface and Colloid Science, Marcell Dekker, New York, 2002, pp. 314–345.
[17] Y. Feldman, I. Ermolina, Y. Hayashi, Time domain dielectric spectroscopy study of biological systems, IEEE Trans. Diel. Elect. Ins. 10 (2003) 728–753.
[18] Y. Polevaya, I. Ermolina, M. Schlesinger, B.-Z. Ginzburg, Y. Feldman, Time domain dielectric spectroscopy study of human cells. II — normal and malignant white blood cells, Biochim. Biophys. Acta 1419 (1999) 257–271.
[19] C. Gabriel, S. Gabriel, E. Corthout, The dielectric properties of biological tissues: I — literature survey, Phys. Med. Biol. 41 (1996) 2231–2249.
[20] M. Sancho, G. Martinez, C. Martin, Accurate dielectric modelling of shelled particles and cells, J. Electrost. 57 (2003) 143–156.
[21] T.M. Shi, S.J.R. Simons, F.J. Dickin, R.A. Williams, Electrical sensing of dispersion behavior, Colloids Surf., A Physicochem. Eng. Asp. 77 (1993) 9–27.
[22] C.L. Davey, G.H. Markx, D.B. Kell, On the dielectric method of monitoring cellular viability, Pure Appl. Chem. 65 (1993) 1921–1926.
[23] C.M. Harris, D.B. Kell, The radiofrequency dielectric properties of yeast cells measured with a rapid automated frequency domain dielectric spectrometer, Bioelectrochem. Bioenerg. 11 (1983) 15–28.
[24] V. Raicu, N. Kitagawa, A. Irimajiri, A quantitative approach to the dielectric properties of the skin, Phys. Med. Biol. 45 (2000) L1–L4.
[25] V. Raicu, T. Saibara, A. Irimajiri, Multifrequency method for dielectric monitoring of cold-preserving organs, Phys. Med. Biol. 45 (2000) 1397–1407.
[26] J. Lei, J.T.K. Wan, K.W. Yu, H. Sun, First principle approach to dielectric behavior of non-spherical cell suspensions, Phys. Rev. E 64 (2001) 012903-1/4.
[27] K. Asami, Effects of membrane distruption on dielectric properties of biological cells, J. Phys. D: Appl. Phys. 39 (2006) 4654–4663.
[28] K. Asami, Dielectric dispersion in biological cells of complex geometry simulated by the three dimensional finite difference method, J. Phys. D: Appl. Phys. 39 (2006) 492–499.
[29] K. Sekine, N. Torii, C. Kuroda, K. Asami, Calculation of dielectric spectra of suspensions of rod-shaped cells using boundary element method, Bioelectrochem. 57 (2002) 83–87.
[30] K. Sekine, Y. Watanabe, S. Hara, K. Asami, Boundary-element calculation for dielectric behavior of doublet-shaped cells, Biochim. Biophys. Acta 1721 (2005) 130–138.
[31] K. Sekine, C. Kuroda, N. Torii, Boundary-element calculation for dielectric relaxation of water-in-oil-in-water emulsions consisting of spherical droplets with a spheroidal core, Colloid Polym. Sci. 280 (2002) 71–77.
[32] K. Sekine, Application of boundary element method to calculation of the complex permittivity of suspensions of cells in shape $D_{\infty h}$ symmetry, Bioelectrochemistry 52 (2000) 1–7.
[33] K. Asami, T. Hanai, N. Koizumi, Dielectric approach to suspensions of ellipsoidal particles covered with a shell in particular reference to biological cells, Jpn. J. Appl. Phys. 19 (1980) 359–365.
[34] E. Gheorgiu, Measuring living cells using dielectric spectroscopy, Bioelectrochem. Bioenerg. 40 (1996) 133–139.
[35] D. Vrinceanu, E. Gheorgiu, Shape effects on the dielectric behaviour of arbitrarily shaped particles with particular reference to biological cells, Bioelectrochem. Bioenerg. 40 (1996) 167–170.
[36] A. Gray, Cassini ovals, Modern Differential Geometry of Curves and Surfaces with Mathematica, CRC Press, Boca Raton, 1997, pp. 117–123.
[37] E.H. Lockwood, A Book of Curves, Univ. Press, Cambridge, 1967.
[38] J.L. Sebastian, S. Munoz San Martin, M. Sancho, M. Miranda, Erytrocyte rouleau formation under polarized electromagnetic fields, Phys. Rev. E 72 (2005) 091923-1/9.
[39] P.B. Canham, The minimum energy of bending as a possible explanation of the biconcave shape of the human red blood cells, J. Theor. Biol. 26 (1970) 61–81.
[40] E. Gheorghiu, On the limits of ellipsoidal models when analyzing dielectric behavior of living cells, Ann. N. Y. Acad. Sci. 873 (1999) 262–268.
[41] V. Kralj-Iglič, S. Svetina, B. Žekč, The existence of non-axisymmetric bilayer vesicle shapes predicted by the bilayer couple model, Eur. Biophys. J. 22 (1993) 97–103.
[42] E. Evans, Y.C. Fung, Improved measurements of the erytrocyte geometry, Microvasc. Res. 4 (1972) 335–347.
[43] A. Di Biasio, C. Cametti, Effect of the shape of human erythrocytes on the evaluation of the passive electrical properties of the cell membrane, Bioelectrochemistry 65 (2005) 163–169.
[44] K. Asami, T. Yonezawa, H. Wakamatsu, N. Koyanagi, Dielectric spectroscopy of biological cells, Bioelectrochem. Bioenerg. 40 (1996) 141–145.
[45] K. Asami, E. Gheorghiu, T. Yonezawa, Dielectric behavior of budding yeas in cell suspensions, Biochim. Biophys. Acta 1381 (1998) 234–240.
[46] K. Asami, T. Hanai, N. Koizumi, Dielectric analysis of *Escherichia coli* suspension in the light of the theory of interfacial polarization, Biophys. J. 31 (1980) 215–228.
[47] E. Gheorghiu, K. Asami, Monitoring cell cycle by impedance spectroscopy: experimental and theorethical aspects, Bioelectrochem. Bioenerg. 45 (1998) 139–143.
[48] K. Asami, Effect of cell shape on dielectric behavior of fission yeast, Biochim. Biophys. Acta 1472 (1999) 137–141.
[49] A. Irimajiri, M. Ando, R. Matsuuoka, T. Ichinowatabi, J. Takeuchi, Dielectric monitoring of rouleaux formation in human whole blood: a feasibility study, Biochim. Biophys. Acta 1290 (1996) 207–209.